Geophysical Research Letters

RESEARCH LETTER
10.1029/2024GL110424

Key Points:

- High-resolution rainfall data reveal an increasing trend in extreme summertime rainfall, especially from mesoscale convective systems
- More events occurred during summers with greater southerly moisture transport driven by differences in the North Atlantic Subtropical High
- The relatively small scale of extreme convective rainfall presents a challenge for representing these events in weather and climate models

Supporting Information:

Supporting Information may be found in the online version of this article.

Correspondence to:
J. Chiappa,
jchiappa@ou.edu

Citation:
Chiappa, J., Parsons, D. B., Furtado, J. C., & Shapiro, A. (2024). Short-duration extreme rainfall events in the central and eastern United States during the summer: 2003–2023 trends and variability. *Geophysical Research Letters*, *51*, e2024GL110424. https://doi.org/10.1029/2024GL110424

Received 28 MAY 2024
Accepted 6 AUG 2024

Short-Duration Extreme Rainfall Events in the Central and Eastern United States During the Summer: 2003–2023 Trends and Variability

Jason Chiappa[1], David B. Parsons[1], Jason C. Furtado[1], and Alan Shapiro[1]

[1]School of Meteorology, University of Oklahoma, Norman, OK, USA

Abstract Extreme rainfall events (EREs) caused by convection are a major prediction challenge and can lead to deadly flash flooding. This study investigates EREs from 2003 to 2023 over the central and eastern United States using high-resolution (4-km) Stage IV precipitation analyses. EREs were defined where 12-hr accumulations exceeded the 10-year average recurrence interval thresholds. Summertime (June–August) EREs exhibited pronounced interannual variability, but with statistically significant increasing trends in annual frequency, particularly among those caused by mesoscale convective systems. Significant relationships were also found between summertime convective EREs over the central United States and enhanced poleward moisture transport, consistent with a westward expansion of the climatological North Atlantic Subtropical High. This relationship may aid in medium- and long-range forecasting. However, the spatial scale of EREs often included localized or narrow bands of extreme accumulations, revealing significant challenges in the accurate representation of EREs in weather and climate models.

Plain Language Summary Extreme rainfall events often result from slow-moving thunderstorms that drop heavy rain over the same area for several hours, which can cause deadly flash flooding. This study defines an extreme rainfall event where the 12-hr accumulation would only exceed that amount once every 10 years on average, with a focus on the summer months over the central and eastern United States from 2003 to 2023. Our results show a significant increasing trend in the number of extreme events, especially those caused by larger, longer-duration storms. Our use of a high-resolution rainfall data set also revealed that extreme rainfall often occurs due to nighttime thunderstorms producing heavy rainfall over highly localized areas or narrow (20–40 km wide) swaths. These characteristics present a challenge for global weather and climate models. The frequency of these summertime extreme events also significantly varied from year to year. Summers with more extreme events were associated with a greater northward transport of moist air around the western edge of an area of high pressure that extends westward from the Atlantic Ocean. The relationship between this flow pattern and extreme rainfall suggests a possible path for improving forecasts of extreme rainfall.

1. Introduction

Accurate prediction of extreme rainfall events (EREs) is a critical need since ∼23% of the world's population is directly exposed to 1-in-100-year floods (Rentschler et al., 2022). Numerous studies (e.g., Fowler et al., 2021; Kunkel et al., 2013) have proposed that heavy rainfall events are likely to increase due to anthropogenic climate change and an increase in sub-daily EREs caused by convection has been observed (e.g., Lenderink & Van Meijgaard, 2008, 2010; Park & Min, 2017; Westra et al., 2014). Unfortunately, the accurate representation of convection is a challenge for weather and climate models (Reynolds et al., 2019), particularly for nocturnal mesoscale convective systems (MCSs) and elevated nocturnal convection over continental locations (e.g., Becker et al., 2021; Geerts et al., 2017; Tang et al., 2021). This concern is relevant as most warm season EREs have been known to be associated with nocturnal MCSs (e.g., Maddox et al., 1979; Stevenson & Schumacher, 2014).

The need to improve the representation of nocturnal convection is critical as early studies (e.g., Easterling & Robinson, 1985; Wallace, 1975) have shown that convection and heavy rainfall during the summer have a nocturnal maximum over the central Continental United States (CONUS). Nocturnal MCSs have subsequently been found to frequently occur over numerous land masses including northwest Australia (Ackerley et al., 2015), east Asia (Chen et al., 2017), the La Plata Basin of South America (Romatschke & Houze, 2013), and the Sahel in west Africa (Vizy & Cook, 2018). Hence, it is not surprising that accurately forecasting the magnitude and

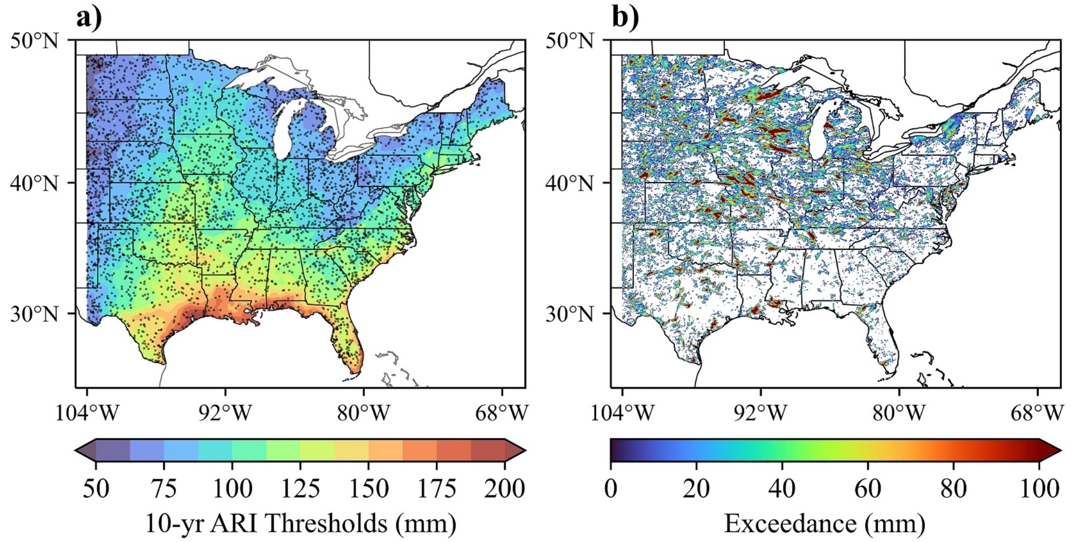

Figure 1. (a) 10-year ARI 12-hr precipitation frequency estimates from NOAA Atlas 14 (color fill; mm) and the locations of all 2003–2023 June–August EREs (not including tropical cyclones and isolated convection) at their respective points of maximum exceedance (translucent black dots). (b) Total precipitation exceeding the 10-year ARI threshold (mm) from all EREs plotted in (a).

location of convective EREs is difficult (e.g., Herman & Schumacher, 2016, 2018; Nielsen & Schumacher, 2016), motivating further exploration of the characteristics (i.e., location, size, structure, and diurnal cycle) of convective EREs and their changes in our warming climate.

This study focuses on EREs over the central and eastern CONUS, where flash flooding from summertime thunderstorms results in the greatest proportion of flood-related fatalities (Ashley & Ashley, 2008), and flooding remains the deadliest storm-related phenomenon in the nation (NWS/NOAA, 2023). Previous observational studies have documented the frequency, seasonal cycle, and location of heavy rainfall events over this region (Brooks & Stensrud, 2000; Hitchens et al., 2013; Maddox et al., 1979; Schumacher & Johnson, 2006; Stevenson & Schumacher, 2014) and the environments associated with these events (e.g., Barlow et al., 2019). These investigations found an annual peak in ERE frequency during the summer [June–August (JJA)], most often associated with MCSs, over large portions of the region. Feng et al. (2016) and Hu et al. (2020) utilized observations to show that the size, duration, and rainfall volume of MCSs across the central CONUS increased during the spring and early summer over the last several decades. Modeling studies (e.g., Prein et al., 2017) suggest that this increase will likely continue in a future climate.

Our study (Further details on the initial methods and findings of this investigation can be found in Chiappa (2023)) explores the characteristics of convective EREs over the central and eastern CONUS from 2003 to 2023 using the high-resolution gridded multi-sensor Stage IV precipitation data set (Lin & Mitchell, 2005). We examine the seasonal/diurnal cycle, structure of accumulation swaths, and temporal variations in frequency and severity of these EREs. We also analyze the large-scale meteorological patterns that correlate with more frequent and/or intense EREs during the summer.

2. Methods

2.1. Defining EREs

EREs were defined where the 12-hr accumulated precipitation derived from hourly Stage IV data exceeded the location's 10-year average recurrence interval (ARI) threshold (Figure 1a). The thresholds were defined using the NOAA Atlas 14 data set (Perica et al., 2018), linearly interpolated onto the 4-km Stage IV grid for the CONUS east of 104°W, avoiding the terrain of the Rocky Mountains. Our algorithm iteratively sums the previous 12 hr of Stage IV data at each hour before grouping points that exceed the threshold within a radius of 250 km and a timeframe of 12 hr into event objects. This approach enables an evaluation of the diurnal cycle of EREs. The arbitrary radius of

250 km was used initially to separate EREs produced by simultaneous heavy rainfall over different regions. Subsequently, any nearby events with shared exceedance points due to the event spanning beyond the 250-km radius were combined. Maps of exceedance above the 10-year ARI threshold were generated for each event.

The National Weather Service River Forecast Centers (RFCs) process and perform quality control on the Stage IV quantitative precipitation estimates. However, the hourly data generally lack manual quality control (e.g., Nelson et al., 2016) leading to numerous spurious events in our preliminary ERE database. Thus, the summed hourly data were cross-checked with the 6- and 24-hr Stage IV data, which undergo more consistent quality control by the RFCs, and then developed, tested, and applied automated quality control procedures to filter out the remaining spurious events (see Text S1 in Supporting Information S1). A significant decreasing trend in the number of flagged events was observed through our analysis period (Figure S1 in Supporting Information S1), suggesting an improvement in the quality of the Stage IV data set. This apparent change in data quality implies that the data set is inhomogeneous with time, evoking caution in the interpretation of trends in the data (as discussed in Section 6). The events in 2002, the first year of the data set, were not utilized due to numerous unrealistically high precipitation estimates.

Significant spatial variability appeared in the occurrence of EREs (Figure S2 in Supporting Information S1), attributable to natural spatial variations in rainfall as well as errors in the Stage IV data (e.g., Smith et al., 2024), variations in processing techniques across RFC boundaries, and errors in NOAA Atlas 14 thresholds (e.g., Kim et al., 2022). The average number of events per grid point was ∼1.4, when the average should be 2.1 over a period of 21 years with an ARI of 10 years. The lower number of events relative to expectations implies that the Stage IV data may underestimate extreme rainfall amounts over several areas, consistent with earlier studies (e.g., Nelson et al., 2016). Thus, EREs may be underrepresented over some locations.

Since the focus of this study is on organized summertime convection, EREs associated with tropical cyclones and isolated convection were filtered out using automated processes (see Text S2 in Supporting Information S1). The remaining events will be referred to as *filtered EREs*. A total of 4,501 JJA filtered EREs were analyzed with their locations and total exceedance mapped in Figures 1a and 1b, respectively. MCS-related events were defined as a subset of the filtered EREs when the nearest group of contiguous grid points exceeding 1 mm hr^{-1} (i.e., *precipitation feature*) had a major axis length of at least ∼200 km for four or more consecutive hours. These criteria were adapted from Feng et al. (2016). While these EREs may be produced by widespread stratiform precipitation associated with extratropical cyclones or coastal lows, visual inspection revealed that non-convective events were uncommon during JJA, comprising only ∼2% of the total. Thus, filtering out non-convective EREs did not significantly impact our results.

2.2. Analysis

To investigate ERE variability and trends, a time series of annual event counts was generated for various subsets (based on classification, season, time of day, etc.). The time series of total exceedance above the 10-year ARI threshold from all points of exceedance (i.e., *total exceedance volume*) was also generated for the JJA filtered EREs to estimate overall intensity. This metric heavily weights EREs where the ARI threshold was exceeded by a greater margin and/or over a larger region, which have greater potential to produce damage and are less likely a result of localized erroneous data. Consistent with recent studies (e.g., Kunkel et al., 2013; M. Li et al., 2022; Panda & Sahu, 2019), monotonic trends were identified using the nonparametric Mann-Kendall trend test (Mann, 1945) and the magnitudes of such trends were estimated using the Theil-Sen's slope estimator (Sen, 1968; Theil, 1950). To maintain a consistent use of robust statistics, this methodology was used for both exceedance volume and event counts.

The time series of JJA filtered ERE counts and total exceedance volume were also combined by standardizing and averaging both time series to create a metric (*ERE index*) that is representative of both ERE frequency and intensity. To identify large-scale meteorological patterns associated with more active JJAs, the ERE index was used to perform composite and correlation analysis with JJA-averaged fields from the European Center for Medium-Range Weather Forecasts Reanalysis v5 (ERA5; Hersbach et al., 2020). The top and bottom 3 years in the ERE index time series (identified as "*active*" and "*inactive*") were selected for composite analysis, and statistical significance in the composite differences at each grid point was determined using the Monte Carlo bootstrapping method (n = 5,000). Significance thresholds were adjusted to address field significance by controlling the false discovery rate (Wilks, 2016). See Text S3 in Supporting Information S1 for more details.

3. ERE Climatology and Characteristics

About 61% of the total 9,571 EREs in the 21-year database occurred during JJA (Figure S3 in Supporting Information S1), consistent with previous studies. EREs classified as MCS-related comprised ∼51% of the JJA events, which, after filtering out tropical cyclone events, contributed to ∼89% of the total exceedance volume during JJA. About half of the JJA EREs were nocturnal (defined in Text S2 in Supporting Information S1), contributing to ∼68% of the JJA total exceedance volume. The most intense JJA EREs were associated with nocturnal MCSs, consistent with previous studies (e.g., Maddox et al., 1979; Stevenson & Schumacher, 2014). During JJA, EREs caused by widely scattered convection tend to peak in intensity during the late afternoon and early evening hours, while MCS-related EREs have a broader peak lasting into the early morning hours (Figure S4 in Supporting Information S1). This result is relatively consistent with previous studies of the diurnal cycle of warm season extreme rainfall over the central CONUS (e.g., Hitchens et al., 2012, 2013; Schumacher & Johnson, 2006; Stevenson & Schumacher, 2014).

The locations of maximum exceedance for all filtered EREs during JJA (Figure 1a) indicate that numerous events occurred to the north of the higher ARI thresholds found over the Gulf Coast states. The most widespread/intense events (all MCS-related) occurred between the Central Great Plains and the Great Lakes (Figure 1b) with extreme accumulation swaths often having relatively narrow widths (20–40 km), creating a significant challenge for coarse grid weather and climate models.

4. Variability and Trends

The annual time series of the total number of JJA filtered EREs (Figure 2a) reveals significant interannual variability with 274 events in 2016 and only 139 events in 2012. This variability is significantly amplified when examining the time series of total exceedance volume (Figure 2b) with a coefficient of variation of ∼44%, in contrast to ∼16% for ERE counts. A statistically significant increasing trend is observed in the time series of JJA filtered ERE counts ($p_{MK} < 0.05$), with an average increase of ∼17% decade^{-1} based on the Theil-Sen's slope (β_{TS}). The total JJA filtered ERE exceedance volume time series exhibits a stronger relative increase of ∼31% decade^{-1}, suggesting a faster increase in ERE intensity than frequency, but this trend lacks statistical significance due to the high variability. No significant trends were observed during other seasons (Figure S5 in Supporting Information S1) based on our methodology, in contrast to some other studies (e.g., Feng et al., 2016), motivating further investigation of summertime EREs.

In contrast to filtered EREs, a statistically significant *decrease* was found in JJA events from isolated convection (Figure 2c). In addition, when separating the JJA filtered EREs among MCS and non-MCS subclasses, it was found that the increasing trend was dominated by MCS-related events (Figure 2d), with no observed trend in the non-MCS subclass (not shown). This finding suggests a change in the nature of the precipitation features associated with JJA EREs with decreases in isolated convection and increases in widespread and long-lived convection. Indeed, trend values were found to increase as a function of maximum precipitation feature length up to ∼1,200 km (Figure S6 in Supporting Information S1). While the 21-year period is too short to attribute these trends to climate change, previous studies have shown that MCSs are producing heavier rainfall in a warming climate, while non-MCS rainfall is decreasing (e.g., Feng, 2017; Hu et al., 2020; Prein et al., 2017).

Changes were also observed in the diurnal cycle of EREs (Figure S7 in Supporting Information S1), with a statistically significant increasing trend in JJA filtered EREs peaking during the late night and morning hours (0600–1500 UTC). This signal is likely related to an increase in MCS-related events over nearly the entire diurnal cycle given that the proportion of MCS-related EREs is maximized during those same hours (Figure S4b in Supporting Information S1). In fact, >70% of JJA filtered EREs were classified as MCS-related between 0500 and 1600 UTC, consistent with the warm season nocturnal maximum in MCS activity over the central CONUS (e.g., Haberlie & Ashley, 2019). Our analysis suggests a potential increase in extreme rainfall occurring during the late night and morning hours, which has not been highlighted by previous studies.

Regional trend analysis reveals that statistically significant increasing trends in MCS-related EREs were found over the majority of the domain, excluding Florida, the Southern High Plains, and the Northeast (Figure S8 in Supporting Information S1). However, given the small sample sizes of events within limited regional domains, the regional trend results are highly sensitive to adding or subtracting years from the time series, implying the need for a longer data set.

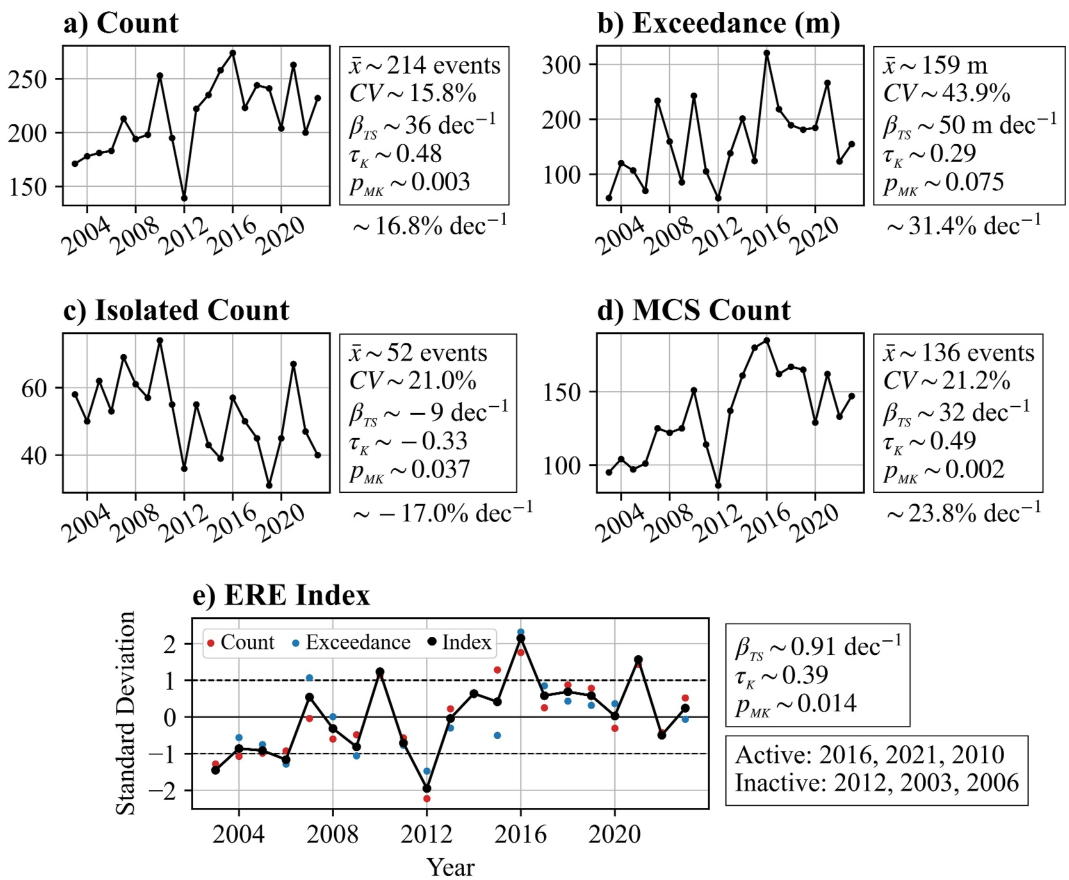

Figure 2. Time series of (a) JJA filtered ERE count, (b) JJA filtered ERE total exceedance volume (m), (c) JJA EREs from isolated convection, (d) JJA EREs from MCSs, and (e) the JJA filtered ERE index (black) with standardized count and exceedance from (a) and (b) (colored points). Statistics, including sample mean ($\bar{x}$), coefficient of variation (CV), Theil-Sen's slope (β_{TS}; decade^{-1}), Kendall's τ (τ_K), the p-value from Mann-Kendall trend tests (p_{MK}), and the average percent change based on the β_{TS} are listed beside each time series.

5. Large-Scale Meteorological Patterns

Next, we utilized ERA5 data to examine how the JJA filtered EREs vary interannually with the characteristics of large-scale meteorological patterns. The ERE index (Figure 2e) was used for composite and correlation analysis, representing both JJA filtered ERE counts and total exceedance volume ($r = 0.9$). The composite analysis was performed for the top (2016, 2021, 2010) and bottom 3 years (2012, 2003, 2006). It is important to note that active summers favored more events occurring over the central CONUS and Ohio Valley, but not over the Southeast and East Coast states (Figure S9 in Supporting Information S1).

Active summers featured significantly higher moisture over the Central Great Plains and Mississippi Valley regions, and strong correlations ($r > 0.7$) with total column water vapor appear across the Southern and Central Great Plains (Figure 3a). Positive correlations with specific humidity are maximized from the surface to around 850 hPa, with correlation coefficients as high as 0.9 over Oklahoma and Kansas. According to numerous studies, periods of heavy rainfall are often associated with anomalously high moisture transport (e.g., Mo et al., 1997), which can be represented by the vertically integrated water vapor flux parameter. Both composite and correlation analyses reveal a statistically significant pattern of northward moisture transport from the Western Gulf Coast to the Midwest (Figure 3b), similar to previous results for periods of heavy rain and flash flooding over the central CONUS (e.g., Abel et al., 2022; Erlingis et al., 2019; Flanagan et al., 2018; Mo et al., 1997). This enhanced moisture transport is consistent with an anomalous anticyclonic circulation around a region of positive composite differences in 850-hPa geopotential heights over the Southeast (Figure 3c). These findings suggest that a westward expansion of the North Atlantic Subtropical High (NASH) likely plays a crucial role in this moisture

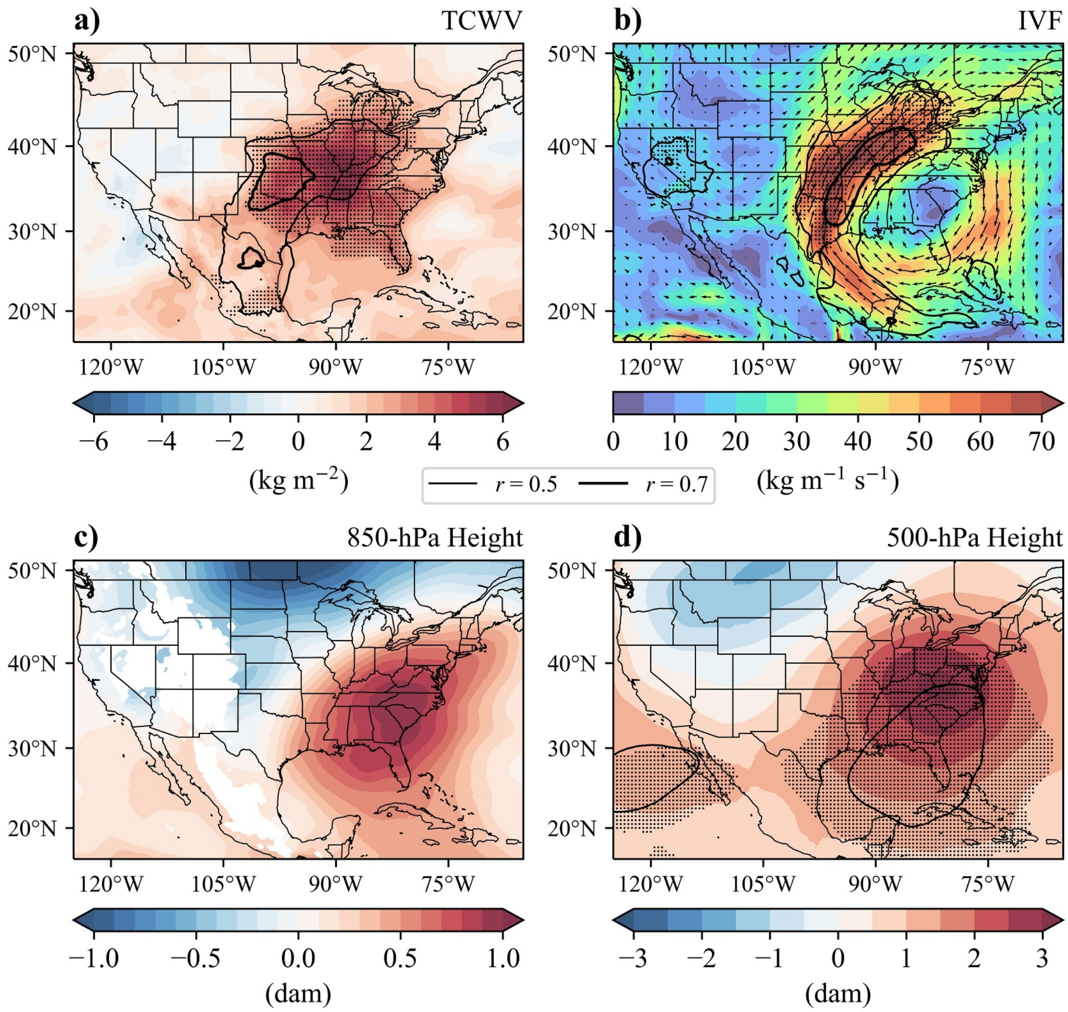

Figure 3. Composite difference between the top three active and inactive years (color fill) in the JJA-averaged ERA5 (a) total column water vapor (kg m^{-2}), (b) vertically integrated vapor flux (kg m^{-1} s^{-1}), (c) 850-hPa geopotential height (decameters), and (d) 500-hPa geopotential height (decameters). Correlation coefficients between the detrended JJA filtered ERE index time series and the respective detrended ERA5 field time series at each grid point are shown as black contours at $r = 0.5$ (moderate correlation; thinner) and $r = 0.7$ (strong correlation; thicker), where applicable. From the 0.25° resolution ERA5 field time series linearly interpolated onto a 0.5° resolution grid (125–65°W, 15–52°N; $N = 9{,}075$ tests), any stippling indicates where the composite difference is statistically significant at the 90% confidence level, accounting for field significance ($\alpha_{FDR} = 0.2$), based on Monte Carlo simulations.

transport and, thus, the occurrence of EREs. However, composite differences and correlations with geopotential height patterns do not become statistically significant until reaching 500 hPa (Figure 3d), suggesting that enhanced mid-level ridging over the eastern CONUS, is a robust signal for more intense EREs over the central CONUS during the summer. Separate composite and correlation maps for Figure 3 and the results for several additional ERA5 fields are available in Supporting Information S1.

6. Discussion and Conclusions

This study introduces a database of short-duration (12-hr) EREs using Stage IV quantitative precipitation estimates. Our approach is similar to the Stevenson and Schumacher (2014) study but extends over a longer period (10 vs. 21 years), uses a newer ARI data set, and derives 12-hr accumulations from hourly Stage IV data with additional quality control. Maps showing swaths of accumulation exceeding the extreme threshold (Figure 1b) reveal that extremes often occur over localized zones or within relatively narrow swaths, the largest of which having widths of 20–40 km associated with MCSs. The narrow banded structure of the extreme accumulation swaths presents a major challenge for numerical models, especially for coarse-grid global weather and climate models with parameterized convection. Thus, utilizing high-resolution convection-permitting models is critical to predict EREs and accurately understand the impacts of climate change on EREs (e.g., Prein et al., 2015).

Nearly 70% of the total JJA extreme rainfall volume (excluding tropical cyclones) was produced from nocturnal convection. This finding provides additional evidence that nocturnal MCSs are the most prevalent producers of extreme rainfall or flash flooding (e.g., Maddox et al., 1979; Stevenson & Schumacher, 2014), further motivating the need to address the major challenge of improving numerical modeling of nocturnal convection (e.g., Geerts et al., 2017; Tang et al., 2021).

Our analysis suggests that EREs associated with MCSs exhibited a statistically significant increase in frequency over most of the central and eastern CONUS from 2003 to 2023 (Figure 2d), while EREs associated with isolated convection exhibited a decrease (Figure 2c). Although the timescale of our study is too short to attribute this increase to anthropogenic climate change, an increase in MCS versus non-MCS rainfall has been both observed and modeled (e.g., Feng et al., 2016; Hu et al., 2020; Prein et al., 2017; Rasmussen et al., 2020). This increase was proposed to be related to increasing moisture and convergence in future MCS environments (e.g., Feng et al., 2016), and the decrease in localized air mass convection could be related to increasing convective inhibition in a warmer troposphere (e.g., Rasmussen et al., 2020). The impact of anthropogenic climate change on regional extreme precipitation remains uncertain (e.g., Lopez-Cantu et al., 2020), but sources of those uncertainties are being addressed (e.g., Deser et al., 2012; Hawkins & Sutton, 2011; Lehner et al., 2020). Trends may also be influenced by natural climate variability, but no significant correlations were found between the ERE time series and commonly used climate indices (e.g., the Pacific Decadal Oscillation).

Unfortunately, radar-based data sets contain temporal heterogeneities due to changes in instrumentation and processing techniques that may impact the detection of extreme rainfall (e.g., Smith et al., 2024). For example, the Next Generation Weather Radar network used to derive rainfall estimates underwent the dual polarization upgrade from 2011 to 2013. In addition, improvements in RFC techniques and radar data resolution are consistent with a decrease in the removal of spurious events over time in our analysis, especially around 2008. Most spurious events were a result of bad rain gauge reports and/or radar artifacts (e.g., Eldardiry et al., 2017) that we found occurred repeatedly over the same locations, particularly over the eastern CONUS. Thus, this change in data quality is nonrepresentative of the full domain. That being said, given the apparent change in character of the time series beyond 2008, the analysis was repeated for the 2008–2023 period (Figures S24 and 25 in Supporting Information S1), yielding a loss of statistical significance in most trends, except for JJA filtered EREs peaking during the 1100–1400 UTC period (not shown). A consensus from Development and Operations Hydrologists at multiple RFCs in the region of interest revealed that the radar upgrades should not have a substantial impact on the Stage IV data, as radar-estimated rainfall fields were gauge-corrected using consistent instrumentation and methodology (e.g., mean field bias correction). Thus, it is unlikely that any apparent discontinuities in the event count time series are solely a product of changes in the data set itself. However, further investigation should be employed into how these temporal heterogeneities could impact the detection of extreme rainfall in the Stage IV product. In addition, we stress the need for a longer-term and more uniform high-resolution precipitation data set in the future to increase the confidence in any observed trends.

Our study also shows that the time series of JJA event counts and total exceedance volume exhibit a substantial amount of interannual variability (Figures 2a and 2b), with some years being over twice as active as others (e.g., 2016 vs. 2012). Summers with higher ERE frequencies and total exceedance volumes indicate the potential for a greater overall risk of flooding from thunderstorms, especially for populations over the central CONUS and the Ohio Valley. Thus, understanding the meteorological factors that distinguish between active and inactive summers is important, potentially aiding in medium- and long-range forecasting.

Unlike most previous studies of extreme events involving multiple hypothesis testing on spatial grids, we applied a false discovery rate correction to the significance levels to account for field significance (Wilks, 2016). This approach reduces the amount of statistical significance in the results. However, even after applying this correction, our composite and correlation analyses reveal a strong connection between EREs and low–mid-level moisture over the Central Great Plains vicinity (Figure 3a) and enhanced vapor flux from the Western Gulf Coast to the Midwest (Figure 3b), consistent with the areas found to be experiencing the most intense EREs during the summer (Figure 1). This pattern of enhanced moisture transport has been previously linked to warm season heavy rainfall over the Midwest and Northern Great Plains (e.g., Abel et al., 2022; Erlingis et al., 2019; Flanagan et al., 2018; Mo et al., 1997), but such a robust correlation with moisture over the Southern and Central Great Plains has not been previously discussed. The enhanced water vapor content over the Southern and Central Great Plains may be an important factor in the production of extreme-rain-producing nocturnal MCSs over the central CONUS via a southwesterly low-level jet originating from that region (e.g., Trier & Parsons, 1993).

The anticyclonic pattern of enhanced moisture transport is likely related to the geostrophic flow that results from higher geopotential heights over the southeastern CONUS relative to the Northern Great Plains and Rockies (Figures 3c and 3d). While the results for 850-hPa heights and wind fields are not statistically significant after accounting for field significance, the pattern would be consistent with a westward extension of the climatological NASH. This extension has previously been linked to enhanced summertime rainfall over the Midwest (Zorzetto & Li, 2021), as it is likely to be associated with a stronger and/or more frequent low-level jet over the Plains and Mississippi Valley. Regarding implications related to climate change, the NASH is projected to expand westward overall in a future climate (e.g., W. Li et al., 2011), suggesting that summertime EREs over the central CONUS may increase in frequency/intensity because of these changes. Additionally, the significant positive differences and correlations in 500-hPa heights over the southeastern CONUS (Figure 3d) suggest a stronger connection between EREs and the deeper flow pattern associated with ridging over that region.

Data Availability Statement

Stage IV data are available from the National Center for Atmospheric Research's Earth Observing Laboratory (Du, 2011). The NOAA Atlas 14 gridded data file was obtained from https://hdsc.nws.noaa.gov/pub/hdsc/data/tx/. Monthly averaged ERA5 data are available from the Climate Data Store (Hersbach et al., 2023a, 2023b). Trend statistics were calculated using the pyMannKendall package (Hussain & Mahmud, 2019). The database of all detected EREs from 2003 to 2023 that passed quality control is provided in Supporting Information S1 (Data Set S1) and the Python code used to generate the database is provided in Chiappa (2024).

Acknowledgments

This research is supported by National Science Foundation (NSF) Grant 10552760, which is focused on advancing our understanding of the nocturnal environment over the Great Plains and nocturnal convective systems. This research has also been supported by the NSF Prediction of and Resilience against Extreme Events (PREEVENTS) program, Grant ICER-1663840. The authors would also like to acknowledge the staff from the NOAA National Weather Service River Forecast Centers of the North Central, Missouri Basin, Arkansas Red-Basin, Lower Mississippi River, and Southeast regional domains, who provided valuable insights concerning changes in the Stage IV data set. We appreciate the suggestions of the reviewers.

References

Abel, B. D., Rajagopalan, B., & Ray, A. J. (2022). Understanding the dominant moisture sources and pathways of summer precipitation in the southeast Prairie Pothole region. *Earth and Space Science*, *9*(3), e2021EA001855. https://doi.org/10.1029/2021EA001855

Ackerley, D., Berry, G., Jakob, C., Reeder, M. J., & Schwendike, J. (2015). Summertime precipitation over northern Australia in AMIP simulations from CMIP5. *Quarterly Journal of the Royal Meteorological Society*, *141*(690), 1753–1768. https://doi.org/10.1002/qj.2476

Ashley, S. T., & Ashley, W. S. (2008). Flood fatalities in the United States. *Journal of Applied Meteorology and Climatology*, *47*(3), 805–818. https://doi.org/10.1175/2007JAMC1611.1

Barlow, M., Gutowski, W. J., Gyakum, J. R., Katz, R. W., Lim, Y. K., Schumacher, R. S., et al. (2019). North American extreme precipitation events and related large-scale meteorological patterns: A review of statistical methods, dynamics, modeling, and trends. *Climate Dynamics*, *53*(11), 6835–6875. https://doi.org/10.1007/s00382-019-04958-z

Becker, T., Bechtold, P., & Sandu, I. (2021). Characteristics of convective precipitation over tropical Africa in storm-resolving global simulations. *Quarterly Journal of the Royal Meteorological Society*, *147*(741), 4388–4407. https://doi.org/10.1002/qj.4185

Brooks, H. E., & Stensrud, D. J. (2000). Climatology of heavy rain events in the United States from hourly precipitation observations. *Monthly Weather Review*, *128*(4), 1194–1201. https://doi.org/10.1175/1520-0493(2000)128<1194:COHREI>2.0.CO;2

Chen, G., Sha, W., Iwasaki, T., & Wen, Z. (2017). Diurnal cycle of a heavy rainfall corridor over East Asia. *Monthly Weather Review*, *145*(8), 3365–3389. https://doi.org/10.1175/MWR-D-16-0423.1

Chiappa, J. (2023). *A 20-year survey of short-duration extreme rainfall events from summertime convection over the central and eastern United States: Climatology, trends, and meteorological patterns* (Master's Thesis). The University of Oklahoma. Retrieved from https://hdl.handle.net/11244/340067

Chiappa, J. (2024). jchiappa/extreme_rainfall: ERE Database [Software]. *Zenodo*. https://doi.org/10.5281/zenodo.13286368

Deser, C., Phillips, A., Bourdette, V., & Teng, H. (2012). Uncertainty in climate change projections: The role of internal variability. *Climate Dynamics*, *38*(3–4), 527–546. https://doi.org/10.1007/s00382-010-0977-x

Du, J. (2011). *NCEP/EMC 4KM gridded data (GRIB) stage IV data. Version 1.0*. UCAR/NCAR—Earth Observing Laboratory. https://doi.org/10.5065/D6PG1QDD

Easterling, D. R., & Robinson, P. J. (1985). The diurnal variation of thunderstorm activity in the United States. *Journal of Applied Meteorology and Climatology*, *24*(10), 1048–1058. https://doi.org/10.1175/1520-0450(1985)024<1048:TDVOTA>2.0.CO;2

Eldardiry, H., Habib, E., Zhang, Y., & Graschel, J. (2017). Artifacts in stage IV NWS real-time multisensor precipitation estimates and impacts on identification of maximum series. *Journal of Hydrologic Engineering*, *22*(5), E4015003. https://doi.org/10.1061/(asce)he.1943-5584.0001291

Erlingis, J. M., Gourley, J. J., & Basara, J. B. (2019). Diagnosing moisture sources for flash floods in the United States. Part I: Kinematic trajectories. *Journal of Hydrometeorology*, *20*(8), 1495–1509. https://doi.org/10.1175/JHM-D-18-0119.1

Feng, Z. (2017). Near doubling of storm rainfall. *Nature Climate Change*, *7*(12), 855–856. https://doi.org/10.1038/s41558-017-0017-5

Feng, Z., Leung, L. R., Hagos, S., Houze, R. A., Burleyson, C. D., & Balaguru, K. (2016). More frequent intense and long-lived storms dominate the springtime trend in central US rainfall. *Nature Communications*, *7*(1), 1–8. https://doi.org/10.1038/ncomms13429

Flanagan, P. X., Basara, J. B., Furtado, J. C., & Xiao, X. (2018). Primary atmospheric drivers of pluvial years in the United States Great Plains. *Journal of Hydrometeorology*, *19*(4), 643–658. https://doi.org/10.1175/JHM-D-17-0148.1

Fowler, H. J., Lenderink, G., Prein, A. F., Westra, S., Allan, R. P., Ban, N., et al. (2021). Anthropogenic intensification of short-duration rainfall extremes. *Nature Reviews Earth & Environment*, *2*(2), 107–122. https://doi.org/10.1038/s43017-020-00128-6

Geerts, B., Parsons, D., Zieglgler, C. L., Weckwerth, T. M., Biggerstaff, M. I., Clark, R. D., et al. (2017). The 2015 plains elevated convection at night field project. *Bulletin of the American Meteorological Society*, *98*(4), 767–786. https://doi.org/10.1175/BAMS-D-15-00257.1

Haberlie, A. M., & Ashley, W. S. (2019). A radar-based climatology of mesoscale convective systems in the United States. *Journal of Climate*, *32*(5), 1591–1606. https://doi.org/10.1175/JCLI-D-18-0559.1

Hawkins, E., & Sutton, R. (2011). The potential to narrow uncertainty in projections of regional precipitation change. *Climate Dynamics*, *37*(1), 407–418. https://doi.org/10.1007/s00382-010-0810-6

Herman, G. R., & Schumacher, R. S. (2016). Extreme precipitation in models: An evaluation. *Weather and Forecasting*, *31*(6), 1853–1879. https://doi.org/10.1175/WAF-D-16-0093.1

Herman, G. R., & Schumacher, R. S. (2018). Money doesn't grow on trees, but forecasts do: Forecasting extreme precipitation with random forests. *Monthly Weather Review*, *146*(5), 1571–1600. https://doi.org/10.1175/MWR-D-17-0250.1

Hersbach, H., Bell, B., Berrisford, P., Biavati, G., Horányi, A., Muñoz Sabater, J., et al. (2023a). ERA5 monthly averaged data on single levels from 1940 to present. *Copernicus Climate Change Service (C3S) Climate Data Store (CDS)*. https://doi.org/10.24381/cds.f17050d7

Hersbach, H., Bell, B., Berrisford, P., Biavati, G., Horányi, A., Muñoz Sabater, J., et al. (2023b). ERA5 monthly averaged data on pressure levels from 1940 to present. *Copernicus Climate Change Service (C3S) Climate Data Store (CDS)*. https://doi.org/10.24381/cds.6860a573

Hersbach, H., Bell, B., Berrisford, P., Hirahara, S., Horányi, A., Muñoz-Sabater, J., et al. (2020). The ERA5 global reanalysis. *Quarterly Journal of the Royal Meteorological Society*, *146*(730), 1999–2049. https://doi.org/10.1002/qj.3803

Hitchens, N. M., Baldwin, M. E., & Trapp, R. J. (2012). An object-oriented characterization of extreme precipitation-producing convective systems in the midwestern United States. *Monthly Weather Review*, *140*(4), 1356–1366. https://doi.org/10.1175/MWR-D-11-00153.1

Hitchens, N. M., Brooks, H. E., & Schumacher, R. S. (2013). Spatial and temporal characteristics of heavy hourly rainfall in the United States. *Monthly Weather Review*, *141*(12), 4564–4575. https://doi.org/10.1175/MWR-D-12-00297.1

Hu, H., Leung, L. R., & Feng, Z. (2020). Observed warm-season characteristics of MCS and non-MCS rainfall and their recent changes in the Central United States. *Geophysical Research Letters*, *47*(6). https://doi.org/10.1029/2019GL086783

Hussain, M., & Mahmud, I. (2019). pyMannKendall: A python package for non parametric Mann Kendall family of trend tests. *Journal of Open Source Software*, *4*(39), 1556. https://doi.org/10.21105/joss.01556

Kim, J., Shu, E., Lai, K., Amodeo, M., Porter, J., & Kearns, E. (2022). Assessment of the standard precipitation frequency estimates in the United States. *Journal of Hydrology: Regional Studies*, *44*, 101276. https://doi.org/10.1016/j.ejrh.2022.101276

Kunkel, K. E., Karl, T. R., Brooks, H., Kossin, J., Lawrimore, J. H., Arndt, D., et al. (2013). Monitoring and understanding trends in extreme storms: State of knowledge. *Bulletin of the American Meteorological Society*, *94*(4), 499–514. https://doi.org/10.1175/BAMS-D-11-00262.1

Lehner, F., Deser, C., Maher, N., Marotzke, J., Fischer, E. M., Brunner, L., et al. (2020). Partitioning climate projection uncertainty with multiple large ensembles and CMIP5/6. *Earth System Dynamics*, *11*(2), 491–508. https://doi.org/10.5194/esd-11-491-2020

Lenderink, G., & Van Meijgaard, E. (2008). Increase in hourly precipitation extremes beyond expectations from temperature changes. *Nature Geoscience*, *1*(8), 511–514. https://doi.org/10.1038/ngeo262

Lenderink, G., & Van Meijgaard, E. (2010). Linking increases in hourly precipitation extremes to atmospheric temperature and moisture changes. *Environmental Research Letters*, *5*(2), 025208. https://doi.org/10.1088/1748-9326/5/2/025208

Li, M., Sun, Q., Lovino, M. A., Ali, S., Islam, M., Li, T., et al. (2022). Non-uniform changes in different daily precipitation events in the contiguous United States. *Weather and Climate Extremes*, *35*, 100417. https://doi.org/10.1016/j.wace.2022.100417

Li, W., Li, L., Fu, R., Deng, Y., & Wang, H. (2011). Changes to the North Atlantic subtropical high and its role in the intensification of summer rainfall variability in the southeastern United States. *Journal of Climate*, *24*(5), 1499–1506. https://doi.org/10.1175/2010JCLI3829.1

Lin, Y., & Mitchell, K. E. (2005). The NCEP stage II/IV hourly precipitation analyses: Development and applications. In *85th AMS Annual Meeting, American Meteorological Society—Combined Preprints*. Retrieved from https://ams.confex.com/ams/pdfpapers/83847.pdf

Lopez-Cantu, T., Prein, A. F., & Samaras, C. (2020). Uncertainties in future U.S. Extreme precipitation from downscaled climate projections. *Geophysical Research Letters*, *47*(9), e2019GL086797. https://doi.org/10.1029/2019GL086797

Maddox, R. A., Chappell, C. F., & Hoxit, L. R. (1979). Synoptic and meso-scale aspects of flash flood events. *Bulletin of the American Meteorological Society*, *60*(2), 115–123. https://doi.org/10.1175/1520-0477-60.2.115

Mann, H. B. (1945). Nonparametric tests against trend. *Econometrica*, *13*(3), 245. https://doi.org/10.2307/1907187

Mo, K. C., Paegle, J. N., & Higgins, R. W. (1997). Atmospheric processes associated with summer floods and droughts in the central United States. *Journal of Climate*, *10*(12), 3028–3046. https://doi.org/10.1175/1520-0442(1997)010<3028:APAWSF>2.0.CO;2

Nelson, B. R., Prat, O. P., Seo, D. J., & Habib, E. (2016). Assessment and implications of NCEP stage IV quantitative precipitation estimates for product intercomparisons. *Weather and Forecasting*, *31*(2), 371–394. https://doi.org/10.1175/WAF-D-14-00112.1

Nielsen, E. R., & Schumacher, R. S. (2016). Using convection-allowing ensembles to understand the predictability of an extreme rainfall event. *Monthly Weather Review*, *144*(10), 3651–3676. https://doi.org/10.1175/MWR-D-16-0083.1

NWS/NOAA. (2023). Natural hazard statistics. Retrieved from https://www.weather.gov/hazstat/

Panda, A., & Sahu, N. (2019). Trend analysis of seasonal rainfall and temperature pattern in Kalahandi, Bolangir and Koraput districts of Odisha, India. *Atmospheric Science Letters*, *20*(10), e932. https://doi.org/10.1002/asl.932

Park, I. H., & Min, S. K. (2017). Role of convective precipitation in the relationship between subdaily extreme precipitation and temperature. *Journal of Climate*, *30*(23), 9527–9537. https://doi.org/10.1175/JCLI-D-17-0075.1

Perica, S., Pavlovic, S., St Laurent, M., Trypaluk, C., Unruh, D., & Wilhite, O. (2018). Precipitation-frequency Atlas of the United States Volume 11, Version 2.0. https://doi.org/10.25923/1ceg-5094

Prein, A. F., Langhans, W., Fosser, G., Ferrone, A., Ban, N., Goergen, K., et al. (2015). A review on regional convection-permitting climate modeling: Demonstrations, prospects, and challenges. *Reviews of Geophysics*, *53*(2), 323–361. https://doi.org/10.1002/2014RG000475

Prein, A. F., Liu, C., Ikeda, K., Trier, S. B., Rasmussen, R. M., Holland, G. J., & Clark, M. P. (2017). Increased rainfall volume from future convective storms in the US. *Nature Climate Change*, *7*(12), 880–884. https://doi.org/10.1038/s41558-017-0007-7

Rasmussen, K. L., Prein, A. F., Rasmussen, R. M., Ikeda, K., & Liu, C. (2020). Changes in the convective population and thermodynamic environments in convection-permitting regional climate simulations over the United States. *Climate Dynamics*, *55*(1–2), 383–408. https://doi.org/10.1007/s00382-017-4000-7

Rentschler, J., Salhab, M., & Jafino, B. A. (2022). Flood exposure and poverty in 188 countries. *Nature Communications*, *13*(1), 3527. https://doi.org/10.1038/s41467-022-30727-4

Reynolds, C., Williams, K., & Zadra, A. (2019). WGNE systematic error survey results summary. Retrieved from https://www.wcrp-climate.org/JSC40/12.7b.%20WGNE_Systematic_Error_Survey_Results_20190211.pdf

Romatschke, U., & Houze, R. A. (2013). Characteristics of precipitating convective systems accounting for the summer rainfall of tropical and subtropical South America. *Journal of Hydrometeorology*, *14*(1), 25–46. https://doi.org/10.1175/JHM-D-12-060.1

Schumacher, R. S., & Johnson, R. H. (2006). Characteristics of U.S. extreme rain events during 1999–2003. *Weather and Forecasting*, *21*(1), 69–85. https://doi.org/10.1175/WAF900.1

Sen, P. K. (1968). Estimates of the regression coefficient based on Kendall's Tau. *Journal of the American Statistical Association*, *63*(324), 1379–1389. https://doi.org/10.1080/01621459.1968.10480934

Smith, J. A., Baeck, M. L., Miller, A. J., & Claggett, E. L. (2024). Rainfall frequency analysis based on long-term high-resolution radar rainfall fields: Spatial heterogeneities and temporal nonstationarities. *Water Resources Research*, *60*(3), e2023WR035640. https://doi.org/10.1029/2023WR035640

Stevenson, S. N., & Schumacher, R. S. (2014). A 10-year survey of extreme rainfall events in the central and eastern United States using gridded multisensor precipitation analyses. *Monthly Weather Review*, *142*(9), 3147–3162. https://doi.org/10.1175/MWR-D-13-00345.1

Tang, S., Gleckler, P., Xie, S., Lee, J., Ahn, M. S., Covey, C., & Zhang, C. (2021). Evaluating the diurnal and semidiurnal cycle of precipitation in CMIP6 models using satellite- and ground-based observations. *Journal of Climate*, *34*(8), 3189–3210. https://doi.org/10.1175/JCLI-D-20-0639.1

Theil, H. (1950). A rank-invariant method of linear and polynomial regression analysis, Part I. In *Proceedings of the Royal Netherlands Academy of Sciences of the United States of America*.

Trier, S. B., & Parsons, D. B. (1993). Evolution of environmental conditions preceding the development of a nocturnal mesoscale convective complex. *Monthly Weather Review*, *121*(4), 1078–1098. https://doi.org/10.1175/1520-0493(1993)121<1078:EOECPT>2.0.CO;2

Vizy, E. K., & Cook, K. H. (2018). Mesoscale convective systems and nocturnal rainfall over the West African Sahel: Role of the inter-tropical front. *Climate Dynamics*, *50*(1–2), 587–614. https://doi.org/10.1007/s00382-017-3628-7

Wallace, J. M. (1975). Diurnal variations in precipitation and thunderstorm frequency over the conterminous United States. *Monthly Weather Review*, *103*(5), 406–419. https://doi.org/10.1175/1520-0493(1975)103<0406:dvipat>2.0.co;2

Westra, S., Fowler, H. J., Evans, J. P., Alexander, L. V., Berg, P., Johnson, F., et al. (2014). Future changes to the intensity and frequency of short-duration extreme rainfall. *Reviews of Geophysics*, *52*(3), 522–555. https://doi.org/10.1002/2014RG000464

Wilks, D. S. (2016). "The stippling shows statistically significant grid points": How research results are routinely overstated and overinterpreted, and what to do about it. *Bulletin of the American Meteorological Society*, *97*(12), 2263–2273. https://doi.org/10.1175/BAMS-D-15-00267.1

Zorzetto, E., & Li, L. (2021). Impacts of the North Atlantic subtropical high on daily summer precipitation over the conterminous United States. *Journal of Hydrometeorology*, *22*(7), 1697–1712. https://doi.org/10.1175/JHM-D-20-0242.1

References From the Supporting Information

Benjamini, Y., & Hochberg, Y. (1995). Controlling the false discovery rate: A practical and powerful approach to multiple testing. *Journal of the Royal Statistical Society: Series B*, *57*(1), 289–300. https://doi.org/10.1111/j.2517-6161.1995.tb02031.x

Knapp, K. R., Kruk, M. C., Levinson, D. H., Diamond, H. J., & Neumann, C. J. (2010). The international best track archive for climate stewardship (IBTrACS). *Bulletin of the American Meteorological Society*, *91*(3), 363–376. https://doi.org/10.1175/2009BAMS2755.1

Knapp, K. R., Diamond, H. J., Kossin, J. P., Kruk, M. C., & Schreck, C. J. (2018). International best track archive for climate stewardship (IBTrACS) project, version 4.